World Academy of Science, Engineering and Technology
International Journal of Geological and Environmental Engineering
Vol:11, No:9, 2017

Analysis of the Elastic Energy Released and Characterization of the Eruptive Episodes Intensity's during 2014-2015 at El Reventador Volcano, Ecuador

Paúl I. Cornejo

Open Science Index, Geological and Environmental Engineering Vol:11, No:9, 2017 publications.waset.org/10007862/pdf

***Abstract*—**The elastic energy released through Strombolian explosions has been quite studied, detailing various processes, sources, and precursory events at several volcanoes. We realized an analysis based on the relative partitioning of the elastic energy radiated into the atmosphere and ground by Strombolian-type explosions recorded at El Reventador volcano, using infrasound and seismic signals at high and moderate seismicity episodes during intense eruptive stages of explosive and effusive activity. Our results show that considerable values of Volcano Acoustic-Seismic Ratio (VASR or η) are obtained at high seismicity stages. VASR is a physical diagnostic of explosive degassing that we used to compare eruption mechanisms at El Reventador volcano for two datasets of explosions recorded at a Broad-Band *BB* seismic and infrasonic station located at ~5 kilometers from the vent. We conclude that the acoustic energy E_A released during explosive activity (VASR η = 0.47, standard deviation σ = 0.8) is higher than the E_A released during effusive activity; therefore, producing the highest values of η. Furthermore, we realized the analysis and characterization of the eruptive intensity for two episodes at high seismicity, calculating a η three-time higher for an episode of effusive activity with an occasional explosive component (η = 0.32, and σ = 0.42), than a η for an episode of only effusive activity (η = 0.11, and σ = 0.18), but more energetic.

***Keywords*—**Effusive, explosion quakes, explosive, strombolian, VASR.

I. Introduction

EXPLOSION quakes (EQs) are the signals with clear characteristics that are related to explosive eruptions, i.e. Strombolian or any other more or less bigger. The majority of these signals can be identified by the occurrence of an air wave which is caused by the sonic impulse during an explosion when the expanding gas is accelerated at the vent's exit. It produces a partitioning of the energy on the source, part of the energy travels through the ground as seismic waves, and the other part travels through the atmosphere as acoustic waves or air waves. This wave mainly travels through the air with the sound common velocity (330 m/s), and then, it is coupled again to the ground being recorded by the seismometer [21].

Some events of low frequency (LF) show the same frequency-time behavior like the explosions, but they lack an air phase [20]. It may reflect a common source mechanism for deep LF events and shallow explosions produced [26], [15].

Strombolian activity at volcanoes is characterized by the repetition of low amplitude explosions emitting ash and block and more or less continuous gas emissions. This type of activity is frequently observed at volcanoes, sometimes quasi-permanently like at Stromboli (Italy), Yasur (Vanuatu), El Reventador (Ecuador) and sometimes more occasionally like at Tungurahua (Ecuador) or Etna (Italy) [2].

The volcanic complex El Reventador (-77,6578; -0,0807) (Fig. 1) is located to 90 km eastward from Quito, Ecuador, being one of the most active volcanoes in the volcanic Ecuadorian chain [1]. El Reventador volcano is a young cone with a height of 3562 m asl, it is built in the interior of a caldera which has a horseshoe's shape opened eastward where the valley of the Quijos and Coca rivers are situated [3]. At the summit of the El Reventador volcano, a little elongated crater is highlighted that measures around 150 m of length and 30 m of depth. The crater has an east side cracked which makes easy the escape of lava over the cone's east flank during the eruptions. Almost ever, it is possible to observe continuous fumarolic activity at the crater and over the cone's superior flanks; also, tephra threw out the crater, and blocks of lava cover the cone's slopes [8].

The cone of El Reventador volcano has been built by a moderately explosive activity classified as Strombolian based on the observations of the eruption occurred during April and May of the 1976 [7]. Among the materials ejected, flows of basaltic andesite lava chiefly predominate with some breccias and laharitic deposits. All of those materials lay inside of the caldera, where they tend to conflux and accumulate forming lava's fields, and meaning none important threat to the surrounding area and population. On the other hand, the pyroclastic materials tend to be distributed over a broad area located mainly westwards of the cone according to the wind directions.

In this paper, we analyze the partitioning of the elastic energy released through explosions recorded during the 2014 – 2015 more intense eruptive episodes in order to characterize the eruptive activity and to relate its dynamism with some variables that can influence to the elastic energy released, using a parameter denominated by [17] as VASR that measures the relative partitioning of acoustic and seismic energy during Strombolian eruptions.

P. I. Cornejo is with the Department of Geology, Escuela Politécnica Nacional, Quito, Ecuador (e-mail: paul.cornejo@epn.edu.ec).

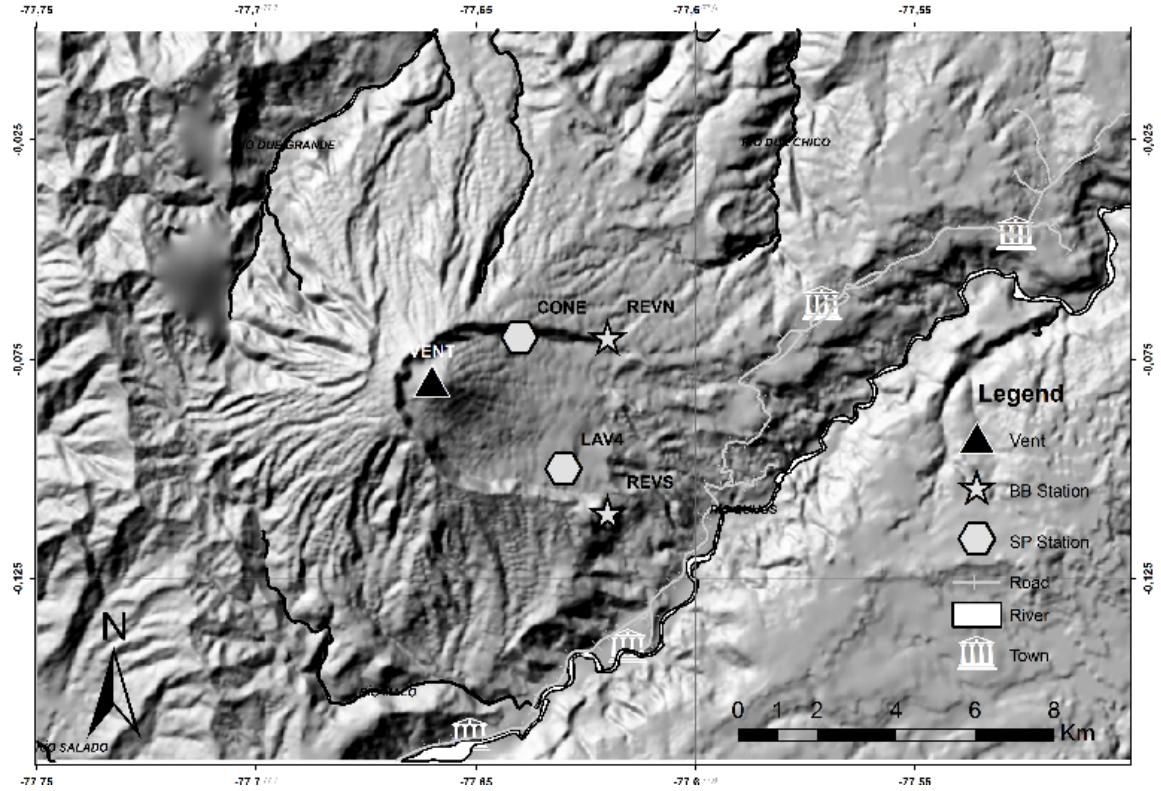


Fig. 1 Location of the seismic stations (Broad Band *BB*, Short Period *SP*), vent, main rivers, roads and towns at El Reventador volcano

II. Background and Data

El Reventador is a stratovolcano that has produced recently some eruptions, e.g. the eruptions occurred in 2002, 2004 – 2006, 2007 and 2008 to the present time, also including several eruptions during the centuries XIX and XX, especially in 1898, 1912, 1926 – 1929, 1944, 1958 – 1960 and 1972 – 1976, and probably other eruptions in the previous centuries which are not described. El Reventador volcano activity is characterized by two types of hazard; the first is related to effusive activity which is about the emission of lava flows, being the main type of eruptive activity. In fact, the lava flows constitute almost the whole cone and the caldera's rock walls [12]. The explosive activity corresponds to the second type of hazard, and according to the latest historic eruptions, these consist fundamentally of ballistic material like bombs, blocks and lava fragments, also ash emission to the atmosphere, being hence related to Strombolian activity. Besides of the formation of pyroclastic flows, the phenomena more frequent linked to the El Reventador's eruptions is the fall of pyroclastic materials with a very variable granulometry. The coarser particles, bombs, blocks, and lapilli fall in the crater's proximity inside a completely uninhabited zone and therefore may constitute a hazard only for the people who stay in the surroundings of the crater or to the monitoring instruments that are eventually installed. Pyroclastic materials which are fine-grained can be transported to long distances from the emission center [12]. Others types of phenomena related to El Reventador's eruptive activity are phreatic explosions, landslides, avalanches, lahars, and the emission of volcanic gases.

Active volcanoes are the source of a wide variety of seismic signals. Traditionally, the volcanic earthquakes have been classified based on the seismogram appearance in four different types: high frequency (HF) or type A, LF or type B, explosions (EQs), and volcanic tremor [21]. The events of the paper's interest are the explosions which are recorded as the others signals by monitoring instruments from Instituto Geofísico – Escuela Politécnica Nacional (IG-EPN) installed at the volcano. El Reventador volcano is monitored by three Short – Period *SP* seismic stations (CHAR, CONE, and LAV4), one Broad – Band *BB* seismic station (REVN), one Broad – Band seismic and infrasound station (REVS), two AFM stations (Azuela and Marker), two cameras, one of them located at the Copete's area and the other at the volcano's southeastern flank; also, the volcano is monitored by tiltmeters and temporal stations (Fig. 1).

The REVS station located around 5 km from the vent (Fig. 2) is composed by a Broad – Band *BB* seismic sensor with three components that has a high gain with a rate of 100 samples/second. The station has a Nanometrics Trillium Compact sensor and a Kinemetrics Quanterra Q330S digitizer. Through the data acquired at the REVS station, we analyzed 5655 events corresponding to the explosions recorded at the most intense eruptive episodes during 2014 – 2015.

Open Science Index, Geological and Environmental Engineering Vol:11, No:9, 2017 publications.waset.org/10007862/pdf

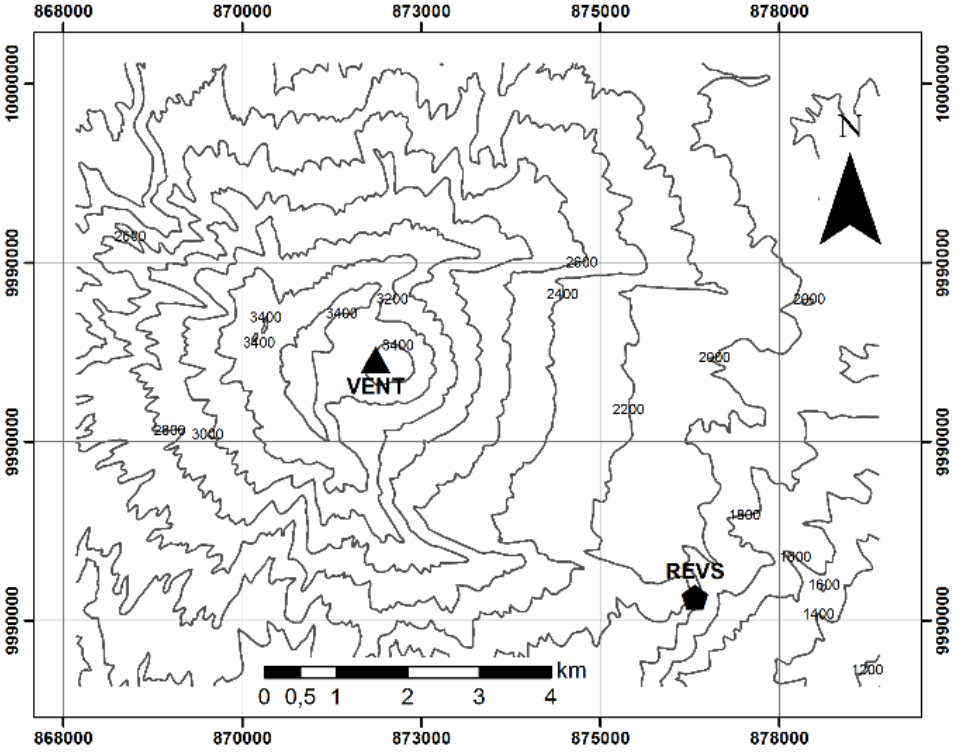


Fig. 2 Location of the Broad Band *BB* seismic and infrasound station REVS (black filled pentagon), and the Vent (black filled triangle)

III. Method

References [16], [17] describe some equations to calculate seismic and acoustic energies, and a parameter "η" named VASR which measures the relative partitioning of elastic energy released. η is helpful to determine relative changes in the volcano's activity, thus the VASR can be used to compare the activity of various volcanoes, or just one, i.e. analyzing a set of data corresponding to one eruption or some eruptions.

For the estimation of acoustic energy, we assume isotropic radiation into the atmosphere (1), so we integrate the entire duration of the acoustic signal in order to quantify the acoustic energy corresponding to discrete Strombolian explosive events. The integral is thus calculated from the signal onset until the time when both seismic and acoustic amplitudes have decayed to background levels. It is important to note that (1) assumes linear sound propagation (infinitesimal excess pressure with respect to ambient pressure) and a monopole source [17].

$$\boldsymbol{E_{acoustic}} = \frac{2\,\pi r^2}{\rho_{atmos}\, c_{atmos}} \int \Delta P(t)^2 dt \qquad (1)$$

For the infrasonic and seismic data presented in this paper, the use of a single station (REVS) is not a significant issue to compare energy estimates for a suite of explosions at a single instrument, assuming a linear system. Furthermore, the raw data (seismic and acoustic) was filtered between 0.5 Hz to 12 Hz by a bandpass filter in order to remove microseism noise and potential Very Long Period (VLP) events contributions.

The parameter of (1) used to determine the *Acoustic Energy* ($E_{acoustic}$ [J]) correspond to: r (r = 5248.85 m) that is the distance from source to receiver, ρ_{atmos} (ρ_{atmos} = 0.914 kg/m^3) is the atmospheric density, c_{atmos} (c_{atmos} = 342.09 m/s) is the average acoustic wave velocity, ΔP (explosion dependent [Pa]) is the excess pressure amplitude, and t (explosion dependent [s]) is the explosion duration time.

Seismic energy propagated into the ground is always more difficult to estimate than the radiated infrasonic energy into the atmosphere, even if the station is located closer or not from the vent. Despite of the elastic propagation, Green's functions are considerably more complex, particularly in the complicated impedance structures common in volcanic systems [17], e.g. El Reventador volcano. An additional complication is that the seismic field includes body and surface waves. Furthermore, strong seismic site responses created by near-surface conditions are common, e.g. in [24]. Acknowledging these difficulties, [17] adopts an approach that assumes that velocity waveforms are representative of the seismic kinetic energy density at a specific location on the volcano. An elastic energy equation analogous to (1), for an isotropic source, is written as [17]:

$$\boldsymbol{E_{seismic}} = 2\pi r^2 \rho_{earth} c_{earth} \frac{1}{A} \int S^2\, U(t)^2 dt \qquad (2)$$

Equation (2) incorporates corrections for *seismic site response* (S = 1) which is fixed at unity for the datasets analyzed in this paper, and an *attenuation* (A = 0.39). To calculate the *Seismic Energy* ($E_{seismic}$ [J]) associated with an EQ for discrete Strombolian events, we integrate the entire duration, picking from the seismic signal onset until the time when seismicity returns to background levels. The interval

Open Science Index, Geological and Environmental Engineering Vol:11, No:9, 2017 publications.waset.org/10007862/pdf

integrated may include one or more discrete pulses as well as extended-duration tremor-like signal [17]. Furthermore, the parameters calculated to (2) are: r (r = 5248.85 m) that is the *distance from source to receiver*, ρ_{earth} (ρ_{earth} = 2380 kg/m^3) is the *volcano density*, c_{earth} (c_{earth} = 3500 m/s) is the *P-wave velocity*, U (*explosion dependent* [m/s]) is the *particle velocity* and t (*explosion dependent* [s]) is the *explosion duration time*.

For the data presented here, which is recorded at sites more than 2 km from the vent, we do a proper assessment of attenuative energy loss. The *attenuation A* of a wave may be expressed by (3). Where f (f = 2 Hz) is the *wave frequency* determined from the analysis of almost 30000 explosions (Fig. 3) and Q (Q = 10) is a *quality factor* assumed from the material composition of the El Reventador volcano structure which is a complex volcanic system.

$$\boldsymbol{A(r)} = e^{\frac{-\pi f r}{c_{earth} Q}} \tag{3}$$

References [17] and [16] enounce that "using estimates of both *acoustic energy* E_A and *seismic energy* E_S, we can characterize the relative partitioning of elastic energy into the atmosphere and into the solid earth by introducing a *volcanic acoustic – seismic ratio VASR* (4). *VASR* is a non-dimensional parameter that may provide insight into the evolving eruption source, magma characteristics, or conduit geometry for explosive eruptions.

$$\boldsymbol{\eta} = \frac{E_A}{E_S} \tag{4}$$

The rapid changes in *VASR* suggest that the variations are source-related and not due to changeable atmospheric structure, which presumably occurs over longer time scales. Furthermore, a trend which shows a correlated increase of both *seismic* and *acoustic energies*, is attributed to variations in explosive yield (eruption magnitude).

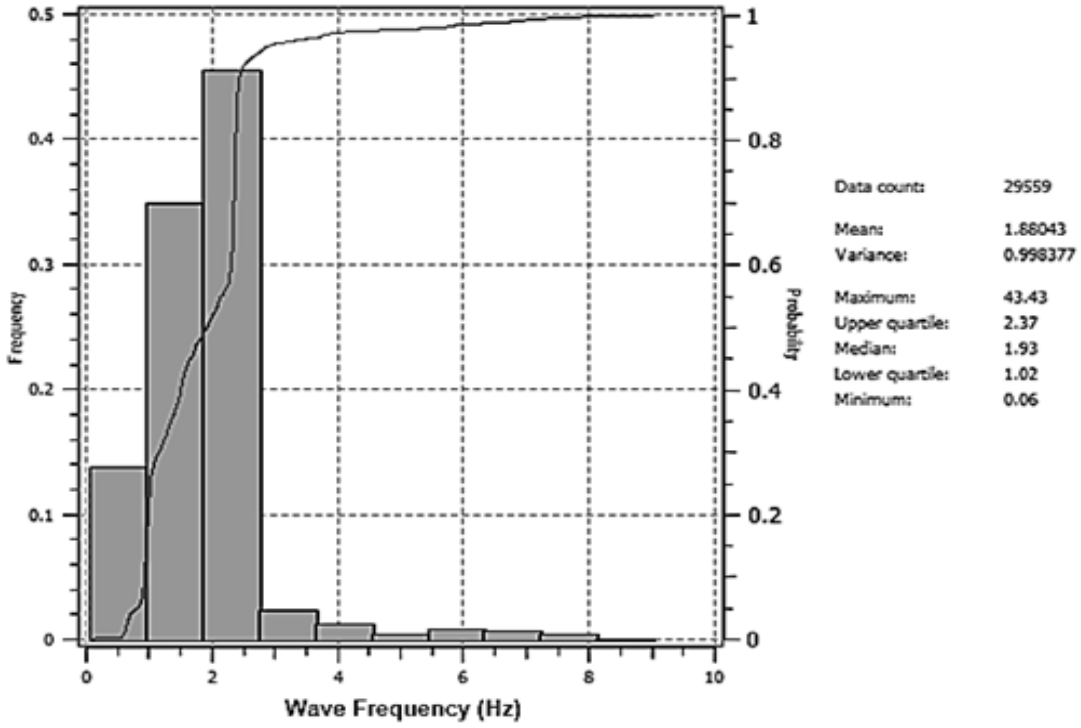


Fig. 3 Histogram of the *wave frequency* (Hz) corresponding to the explosions recorded at El Reventador volcano during 2013 – 2016 at the stations CONE, LAV4, REVN and REVS

Reference [22] examined explosive eruptions at Langila volcano which is located in Papua New Guinea, comparing seismic displacements (Reduced Displacements) with the amplitudes of associated air phases (Reduced Acoustic Pressures) (5). [23] observed that the ash-rich explosive eruptions at Stromboli volcano, Italy were almost ever associated with relatively low-amplitude seismic signals, and hence, [23] proposed that "less ground shaking occurs during a well-formed vertical eruption because less ejecta momentum is imparted laterally to the wall rocks".

$$\boldsymbol{\eta'} = \frac{R_P}{R_D} \tag{5}$$

Equation (5) is another way used to obtain a variable VASR, where η' is a *volcanic acoustic – seismic ratio* [Pa/cm^2], R_P is the *reduced acoustic pressure* [Pa], and R_D is the *reduced displacement* [cm^2].

IV. Intense Eruptive Activity during 2014

A. Eruptive Activity during March – July

Reference [6] details a period of high seismicity which occurred between 25 March and 13 April 2014, with daily recordings for seismic events of 40-103 LPs, 10-30 explosions, 6-195 emission tremor episodes, and 2-55 harmonic tremor episodes. Elevated activity that began on 25

Open Science Index, Geological and Environmental Engineering Vol:11, No:9, 2017 publications.waset.org/10007862/pdf

Open Science Index, Geological and Environmental Engineering Vol:11, No:9, 2017 publications.waset.org/10007862/pdf

March 2014 at 15h00 Local Time *LT* was characterized by a sustained emission tremor gas emission, containing variable amounts of ash, and ejected material being deposited around the crater. Also, partial dome collapse caused pyroclastic flows down the E, SE and S flanks, travelling up to 1.5 km from the summit. And at least two lava flows were observed descending ~500 m from the crater along the E and SE flanks.

From 27 March to 11 April 2014 [6], numerous lava flows were observed. On 27 March, a lava flow on the S flank was observed by IG-EPN video cameras, whereas on 29 March hot spots on the S flank were captured through thermal images. In the morning of 31 March, after a large roar was reported, incandescent material and lava flows traveled around 1 km down the south flank. During the morning of 2 April, lahars produced by rainfall were reported. And, four lava flows on the S and SE flanks were observed on 3 April and continued to be active through 8 April [6]. On 9 and 11 April, lava flows were also reported by IG-EPN, descending through the SW flank.

During the moderate to high seismicity episode of 14 April – 2 May [6], a small pyroclastic flow descended a few meters below the crater, and on 2 May, lava flows on the S and SE flanks were captured by thermal cameras. On the night of 4 May at 20h40 LT, a sizeable explosion ejected a great quantity of incandescent material which descended most of El Reventador's flanks. Furthermore, on the night of 17 June, infrared cameras detected the descent of incandescent material on the S and E flanks. And, on 19 June, incandescent material moved down, but by the NE flank. IG-EPN reported also that day an emission plume.

At 06h50 LT on 2 July, a large explosion produced a considerable plume with moderate amounts of ash which subsequently collapsed and formed a pyroclastic flow that moved about 1.5 km down the S flank [6]. Another explosion was reported, which released a column of vapor and ash that rose to an altitude of 5.6 km and drifted SE. On 3 July, there were 42 LP events recorded, which was higher than the number of LPs recorded on 1 and 2 July (18 and 27, respectively) [6]. Furthermore, during the evening of 26 July, an explosion formed a pyroclastic flow which traveled almost 1 km down the SW flank.

V. Intense Eruptive Activity during 2015

A. Eruptive Activity through March

In the early morning of 11 March, through a thermal camera a new lava flow was observed, that was moving down the SW from the crater overpassing ~500 m down the summit. On 13 March, the lava's flow length was around 1500 m, and the lava flow was moved down in the same direction towards SSW. It is essential to indicate that the seismic activity related to this process had same characteristics as the previous eruptive activity mentioned. Furthermore, IG-EPN reported short-height gas emissions associated to this lava flow [9].

B. Eruptive Activity through May

Images of the thermal camera located at Copete captured the presence of a lava flow which descended from the S flank, recording on 19 May a lava flow with a length over the 1000 m from the summit [10].

On 17 May at 13h50 Coordinated Universal Time *UTC* (08h50 LT) an increase in the amplitude's emission tremor (Fig. 4) related to the extrusion of a lava flow was appreciated in the seismograms. Unfortunately, the weather conditions that dominated those days did not allow to relate directly with the increase of the tremor activity and the beginning of the lava's flow descent. When the weather conditions changed, steam columns and gases of short height (less than 500 m) emitted were observed.

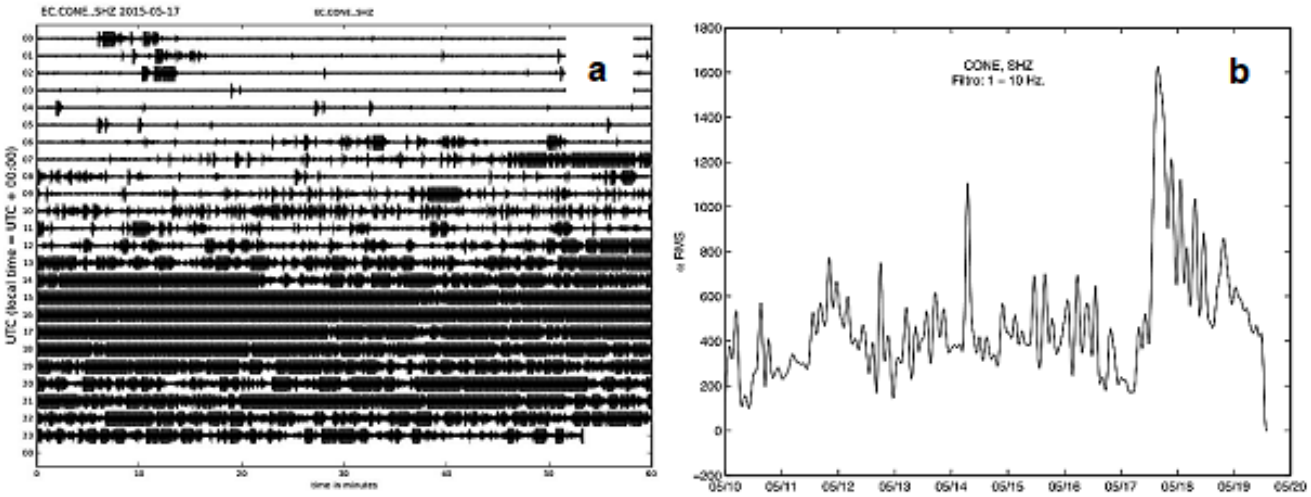


Fig. 4 (a) Seismogram of the CONE station, which is located at the NE flank, shows an important and sustained increase in the tremor's amplitude since 13h50 UTC on 17 May. (b) Evolution of the seismic amplitudes recorded from 10/05/2015 – 19/05/2015, noticing an important increase on 17 May amplitudes and a posterior decrease. Taken and edited from [10]

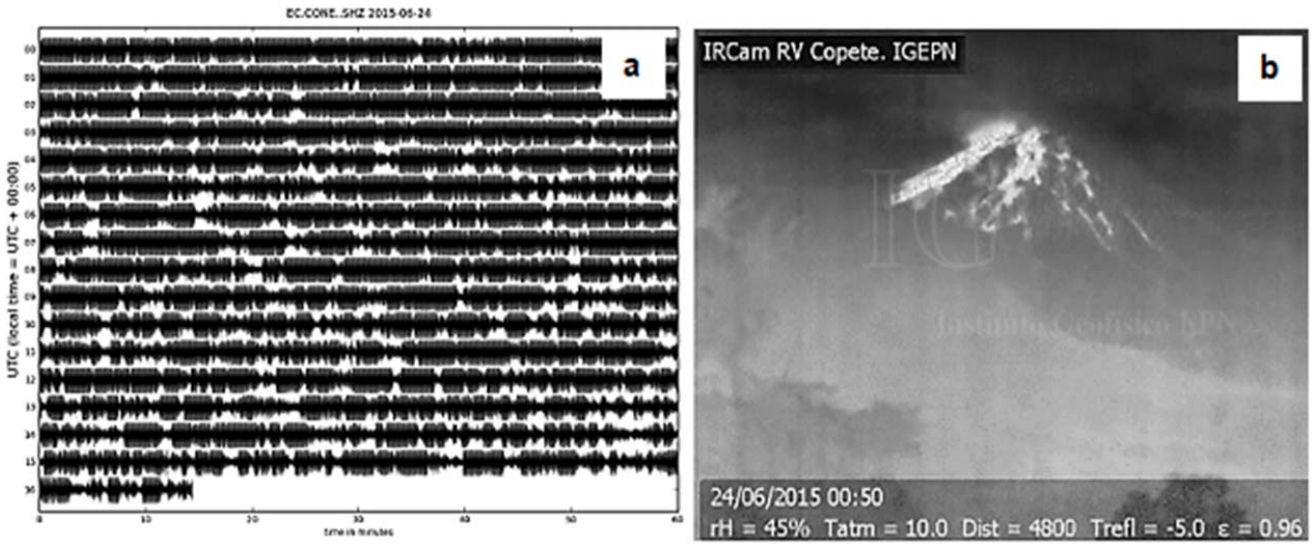


Fig. 5 (a) Seismogram of the CONE station shows a high and sustained tremor activity on 24 June. (b) Thermal infrared image captured at 00h50 UTC on 24 June shows new lava flows descending from the S flank. Taken and edited from [11]

C. Eruptive Activity through June

Similar to the 19 May 2015 activity occurred, at 14h00 UTC (09h00 LT) on 23 June El Reventador volcano produced an increase in the seismic activity characterized by a continuous tremor signal which remained for a long time (Fig. 5 (a)). Furthermore, images captured by the thermal camera located at El Copete indicate that the surface activity also increased and was characterized by various lava flows which descended from the SW, S, and E flanks. The lava flow that moved down the E flank overpassed 1000 m of length (Fig. 5 (b)) [11].

The seismic tremor signal recorded may be related to the eruption of the lava flows mentioned, but due to the persistent cloudy atmosphere at El Reventador volcano, not was possible directly to relate the beginning of the tremor signal with the beginning of the lava's flows eruption. Furthermore, several signals of explosions which accompanied the lava emissions possibly triggered pyroclastic flows.

VI. Discussion

According to (4) proposed by [16] as in [17], there are three expected possibilities. 1) $\eta \sim 1$, which means that acoustic energy is similar or equal to seismic energy radiated into the atmosphere and into the ground, respectively. 2) $\eta < 1$, seismic energy radiated into the ground predominates before the acoustic energy radiated into the atmosphere; being source process which dominates this scenario with small EQs. 3) $\eta > 1$, which means that acoustic energy is larger than seismic energy radiated; not being source process so significant. Instead, an important accumulation of gas in the conduit or near the lava surface reach occasionally the lava surface triggering a lava bubble bursting which emits explosions larger than the common ones. These energetic explosions are well-correlated especially with explosive activity and not well-correlated with effusive activity (Fig. 6 (b)), also EQs with a $\eta > 1$ are more frequently expected in high seismicity periods than in low-moderate seismicity periods (Figs. 6 and 7).

Explosive activity is linked to processes which generate steam columns, ash plumes, gases, and ballistic material ejected. Incandescent material at the summit accompanied by emission plumes is considered in this study as a transitory activity between explosive and effusive. On the other hand, effusive activity is linked to processes which generate lava flows. Furthermore, pyroclastic flows can be related to explosive as effusive activity, e.g. the collapse of an ash plume.

Reference [19] concludes that "plume expansion scales very poorly with both seismic and acoustic trace energy and only the initial amplitude of the acoustic signal is perhaps correlated with initial plume rise speeds". For example, the eventual size of eruption plumes at Tungurahua volcano, Ecuador does not appear to be controlled by elevated material accelerations within the conduit, which are the primary influences on elastic energy radiation. The data of this paper highlight the observation realized in [19] and propose that the magnitude of explosive events like ash plumes and steam emissions is related to the accumulation of previous material or gas released by source events that cannot be released as EQs because there are some forces like surface tension or high lava viscosity acting stronger than the gas released and, therefore allowing a gas accumulation inside the conduit or near the lava surface that occasionally trigger some enormous explosions accompanied by ash plume, steam emission, gases or ballistic material ejected with considerable quantities of acoustic energy and low quantities of seismic energy, producing anomalous values of η or values with $\eta > 1$.

Comparative studies between seismic radiation and eruption intensity for suites of discrete explosions at Karymsky [16], [17], Tungurahua [19], and Santiaguito [18] failed to reveal a robust relation. The study of the relative partitioning, named *VASR*, at El Reventador volcano reveals a relation well-correlated between high, moderate, and low seismicity and η,

Open Science Index, Geological and Environmental Engineering Vol:11, No:9, 2017 publications.waset.org/10007862/pdf

which increases with high eruption intensity and decreases with low eruption intensity (Figs. 6 and 7), but there are few events that not act similar or perhaps a better chronology that describes the eruption intensity must be effected by people who are often monitoring the volcanic activity, e.g. a period of moderate seismicity can be accompanied rarely by events of higher magnitude or intensity.

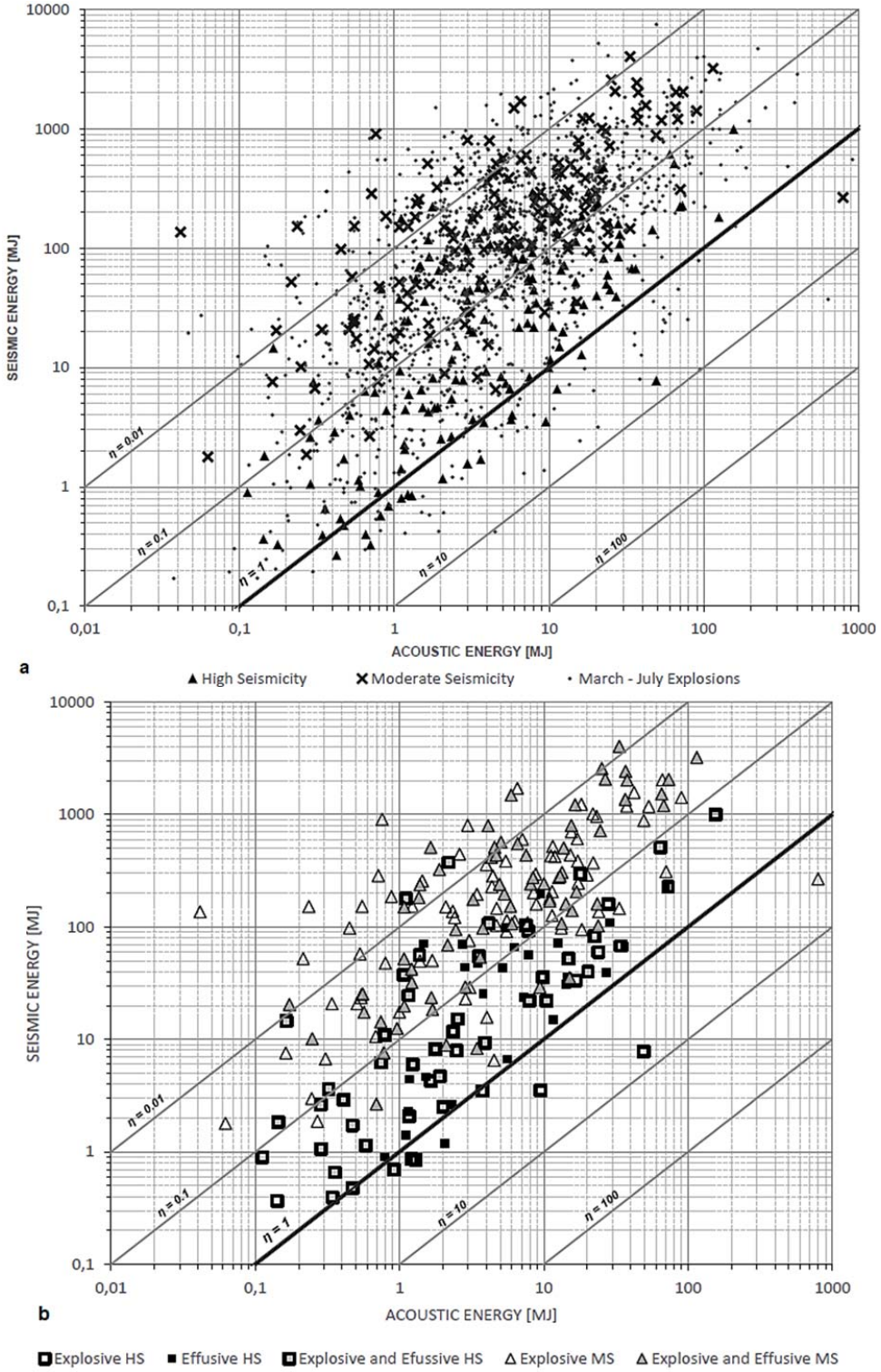


Fig. 6 (a) 1614 Explosions recorded during March – July 2014 are plotted in a log-log graphic. Energy intensity increases rightward and upward. 173 High seismicity *HS* events (black filled triangle), 149 Moderate seismicity *MS* events (black diagonal cross) and 1292 low-high seismicity background events (black dot). (b) 230 Explosions recorded at High and Moderate intensity. 81 High seismicity events (squares) and 149 Moderate seismicity events (triangles). η is referred to *VASR*

Open Science Index, Geological and Environmental Engineering Vol:11, No:9, 2017 publications.waset.org/10007862/pdf

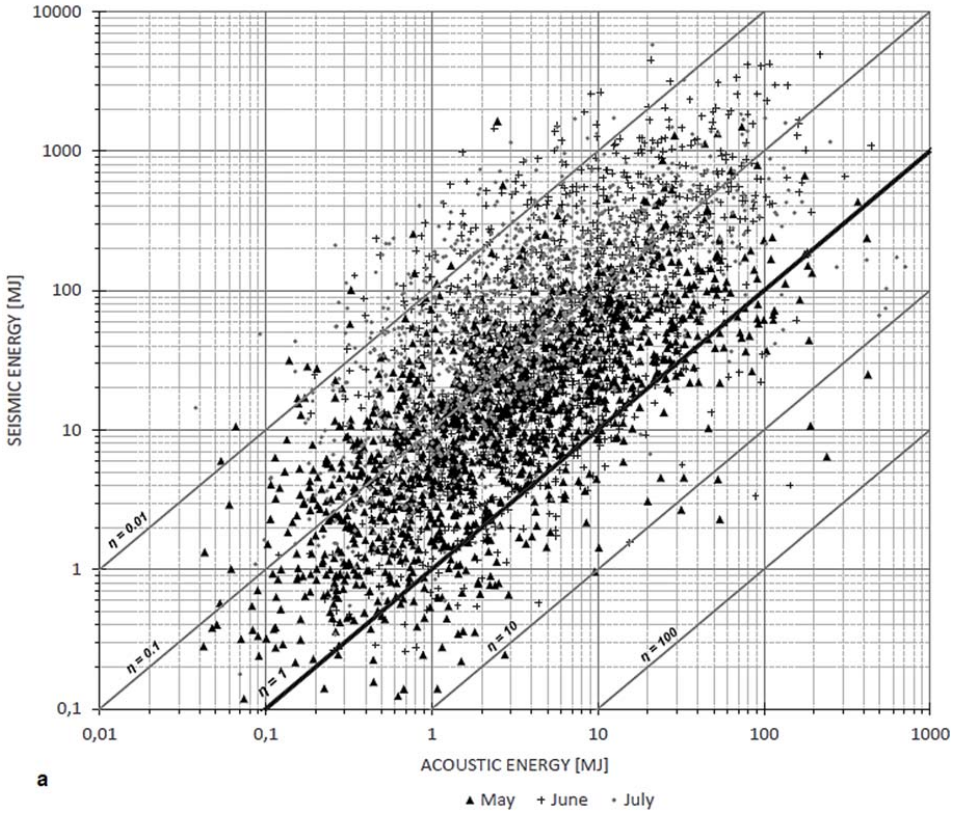
Open Science Index, Geological and Environmental Engineering Vol:11, No:9, 2017 publications.waset.org/10007862/pdf

Most of the explosions reach a η value under 1, being a source process, which dominates the eruptive activity. In general, explosive activity produces η values higher or closer than 1, whereas effusive activity produces η values lower than those reached at explosive activity (Figs. 6 and 7).

We worked with three datasets which correspond to May, June and July 2015 (March does not have data available). May and June are the months with an intense effusive activity level, meanwhile July is a month with background seismicity. Note that June is a period more energetic than May, but with η values are lower than June's ones (Fig. 7). In addition, during the month of May, explosive activity was recorded, whereas June corresponds only to effusive activity.

Reference [27] describes based on their results, a two-stage conceptual model of Strombolian explosions at Aso volcano; the first stage is the vertical ascent of the gas slug within the volcanic conduit before the explosion, and the second stage is the explosion itself. This paper describes the two stages differing that the first stage is related to the gas propagation or gas accumulation and maybe involves explosions of small-moderate size, but the second stage is related to considerable-enormous explosions and also small-moderate sized explosions. [5] Noted that the onset of the higher-frequency signal coincided with the visually observed onset of the eruptive jet, while no visible surface activity could be linked with the precursory low-frequency onset. Therefore, the initial phase of the seismic signal may correspond to the process of ascent of the gas slug to the surface within a conduit, and the main phase of the signal is generated by the explosion at the surface. The similarity of the LF waveforms, may be result of the same way of the slug ascent within the conduit, e.g. Aso volcano [27], whereas some difference in the waveforms of the main phases indicates the difference in the superficial conditions of crater where the explosions occur.

Reference [17] makes a conceptualization of four important variables that may influence *VASR*. 1) *Density-dependent kinetic energy transfer*: a low η is expected when a high density plume (ballistic and entrained ash) is produced, but when a low density plume is produced a high η is expected. 2) *Variable impedance contrasts*: a low η is expected when the lava lake has a high impedance, but a high η is expected with a low impedance lava lake because seismic signals are attenuated. 3) *Viscous flow losses in conduit*: a low η is expected because infrasound signals are diminished due to a long and narrow conduit which implies a deep source and high wall friction, but a high η is expected when the conduit is short and wide because extended-duration and low-amplitude seismic signals are produced. 4) *Source dimension variability*: a low η is expected with a large source region which produces big bubble bursting and diminishes the amplitude of infrasound signals, but with a small source region (monopole approximation) a high η is expected, produced by small-normal bubble bursting. We summarize the activity eruptive intensity at El Reventador volcano in two stages (Fig. 8). a) *Effusive activity* which in general produces a $\eta < 1$ and is characterized for lava flows and small-moderate explosions. b) *Explosive activity* which in general produces a high *VASR* with some values expected of $\eta > 1$ and is characterized for ash plumes, steam emissions, gases and moderate-enormous explosions.



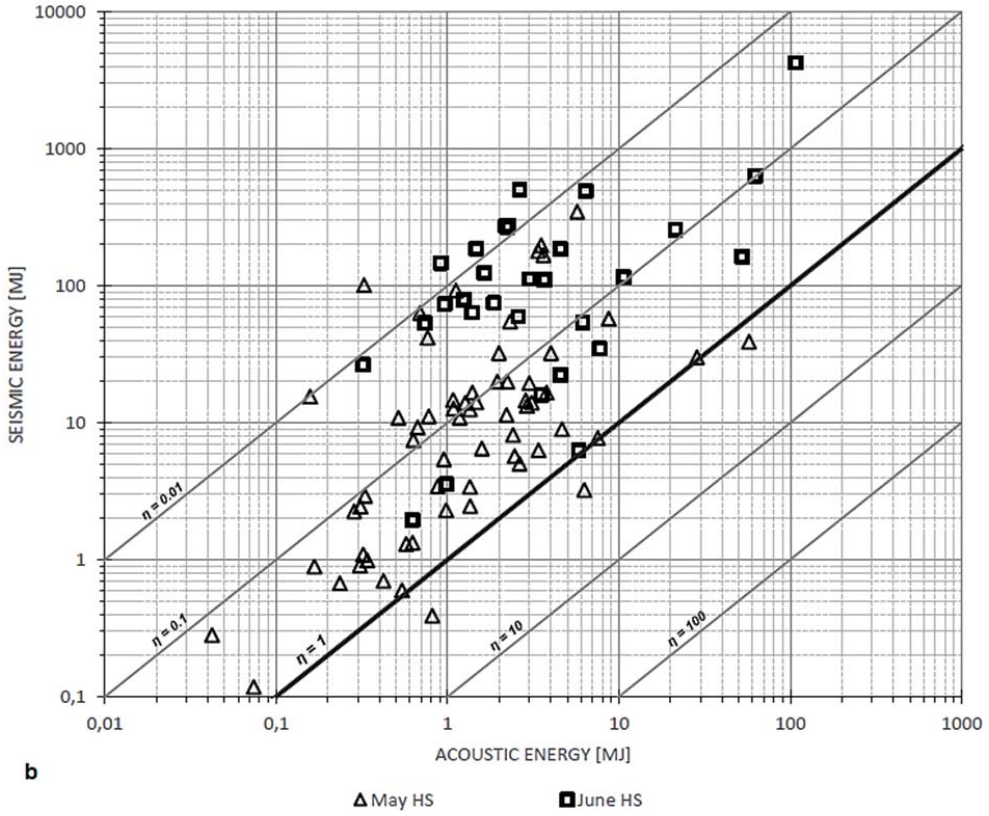


Fig. 7 (a) 4041 Explosions recorded during May, June and July 2015 are plotted in a log-log graphic. Energy intensity increases rightward and upward. 1447 events correspond to May (black filled triangle), 1182 to June (black cross) and 1412 to July (gray circle). (b) 92 explosions recorded at the days of the highest intensity during May and June 2015. 62 explosions correspond to May (triangles) and 30 to June (squares). η is referred to *VASR*

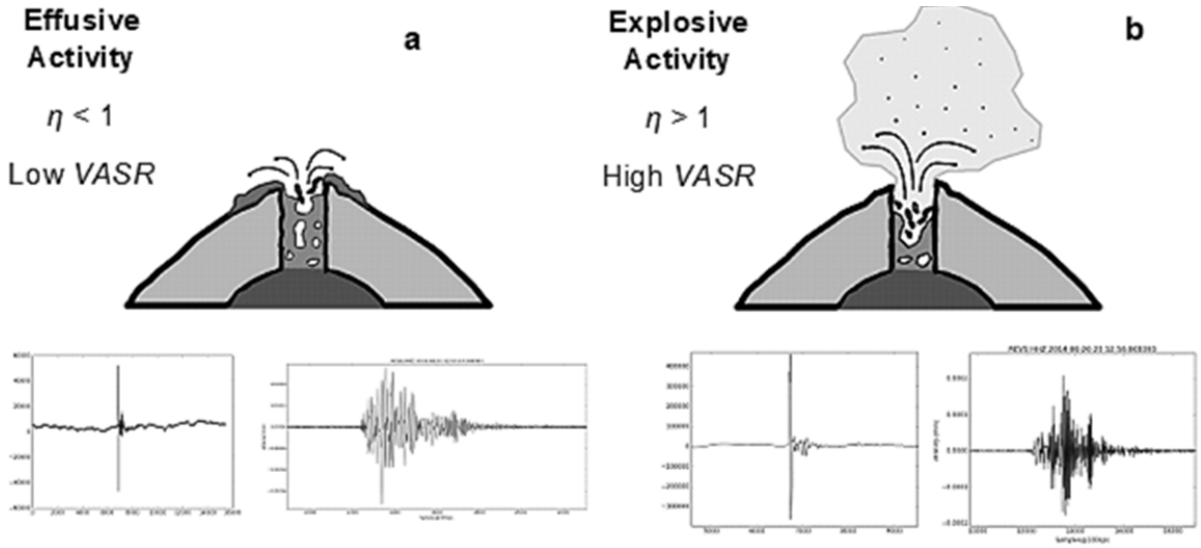


Fig. 8 (a) Sketch illustrating the effusive activity, where $\eta < 1$, below the sketch are acoustic and seismic representative signals of an explosion recorded on 02/04/2014 at 02h58 LT with a $\eta \sim 0.3$ calculated. (b) Sketch illustrating the explosive activity, where $\eta > 1$, below the sketch are acoustic and seismic representative signals of an explosion recorded on 20/06/2014 at 23h15 LT with a $\eta \sim 3$ calculated

Commonly, Strombolian explosions are assumed to be caused by the outburst of gas slugs. In the frame of the model exposed by [2], a tentative explanation would be that LP or LF events are directly related to the propagation of these gas slugs. Such events could occur at specific locations along the conduit such as places where a diameter change is observed [13] or at the top of the magma reservoir where slug coalescence occurs [14]. Alternatively, [2] proposes that LP

Open Science Index, Geological and Environmental Engineering Vol:11, No:9, 2017 publications.waset.org/10007862/pdf

Open Science Index, Geological and Environmental Engineering Vol:11, No:9, 2017 publications.waset.org/10007862/pdf

events may occur independently of the slug propagation, being caused by any pressure fluctuation related to unsteady mass transport [4]. They could be the source of a pressure wave which would propagate upward along the conduit. Gas slug may coalesce independently at shallower depth and their upward propagation could be triggered by the pressure wave. Furthermore, this model could therefore explain the absence of visible EQs after some of the LPs as the pressure wave will not trigger any slug propagation, if the slug coalescence is not sufficiently advanced. Inversely, slug ascent may also occur without the passage of the pressure wave, explaining the absence of any visible LP prior to many explosions.

An optional proposed source process is that there exists a bursting at depth or inside the conduit, and not necessarily each explosion is produced at the surface lava. Experimental models, as in [25], demonstrate that changing the bursting depth in the conduit does not change the scaling of the amplitudes but affects the relative energy partitioning η and the waveform. Being η a parameter that supports the variable energy partitioning, and also some signals recorded and observed in this work with a different waveform to the common ones, both affirmations could confirm a bursting at depth. A study detailing the explosion waveforms and the precursory of EQs is needed to understand more about the gas slug system and the occurrence of different explosion types at El Reventador Volcano.

VII. Conclusion

El Reventador volcano is characterized for being dominated by source processes which produce explosions with a seismic component higher than the acoustic component. It explains a steady degasification and a domain of events with a frequency ~ 2 Hz. However, there is a gas accumulation inside the conduit or at the lava surface. Sometimes, source events do not generate enough gas to produce moderate explosions, producing gas accumulation which aleatory triggers enormous explosions ($\eta > 1$) that are more concurrent in stages of high seismicity and explosive activity. Furthermore, the effusive episode tends to be more energetic than the explosive episode, but the highest η values correspond to explosive events.

We determine, for 2014 eruptive activity episodes, a *VASR* mean value of $\eta = 0.47$, with a standard deviation of $\sigma = 0.8$ corresponding to effusive and explosive activity at high seismicity; being the most intensive eruptive episode, and values of $\eta = 0.08$, and $\sigma = 0.3$ to explosive and ballistic activity at moderate seismicity. During 2015, two stages of high seismicity were analyzed which correspond to effusive activity reported. A *VASR* mean value of $\eta = 0.32$, and $\sigma = 0.42$ correspond to May, a month with occasional explosive activity; and values of $\eta = 0.11$ and $\sigma = 0.18$ correspond to June, a month more energetic than May.

Acknowledgment

The author thanks the Instituto Geofísico, Escuela Politécnica Nacional, Quito, for sharing data available and for bringing help to manage scripts in order to extract data. Specially Hugo Ortiz, Juan Anzieta and Mario Ruiz who were supporting with ideas for the development of this work.

This research did not receive any specific grant from funding agencies in the public, commercial, or not-for-profit sectors.

References

[1] Baby, P., Rivadeneira, M., & Barragán, R. (2014). La Cuenca Oriente: Geología Y Petróleo. Versión Actualizada. Quito: Ifea, Ird, Petroamazonas Ep. 3ra Ed. Edición Especial Conmemorativa Por Los 80 Años De Schlumberger En El Ecuador.

[2] Battaglia, J., Métaxian, J.-P., & Garaebiti, E. (2016). Short term precursors of Strombolian explosions at Yasur volcano (Vanuatu). Geophysical Research Letters, No 43, doi: 10.1002/2016GL067823., 1-6.

[3] Bourquin, J., Samaniego, P., Ramón, P., Bonadonna, C., Kelfoun, K., Vallejo, S., Mothes, P. (2011). Mapas De Los Peligros Potenciales Del Volcán Reventador. Quito: IG-EPN.

[4] Chouet, B., Dawson, P., & Martini, M. (2008). Shallow-Conduit Dynamics at Stromboli Volcano, Italy, Imaged From Waveform Inversions. Geological Society, London, Special Publications, 307 doi:10.1144/SP307.5, 57-84.

[5] Chouet, B., Saccorotti, G., Martini, M., Dawson, P., De Luca, G., Milana, G., & Scarpa, R. (1997). Source and path effects in the wave fields of tremor and explosions at Stromboli Volcano, Italy. JOURNAL OF Geophysical Research, Vol. 102, 15129-15150.

[6] GVP. (2014). Reventador (Ecuador) Ongoing ash emissions, lava flows, and pyroclastic flows through July 2014. Global Volcanism Program. Report on Reventador (Ecuador). In: GVP Staff (ed.), Bulletin of the Global Volcanism Network, 39:7. Smithsonian Institution. Retrieved 4 March 2017 from: http://dx.doi.org/10.5479/si.GVP.BGVN201407-352010.

[7] Hall, M. (1977). El Volcanismo en el Ecuador. Quito: Inst. Pan. Geog. Hist.

[8] Hall, M. (1980). El Reventador, Ecuador, Un Volcán Activo De Los Andes Septentrionales. Politécnica, Monografía De Geología. Vol. V, No 2, 123-136.

[9] IG-EPN. (2015). Informe Especial del Volcán Reventador N°1, 2015. Evaluación de la actividad eruptiva del volcán Reventador. Quito: Escuela Politecnica Nacional. Instituto Geofisico. Retrieved 5 March 2017 from: http://igepn.edu.ec/servicios/noticias/959-informe-especial-del-volcan-reventador-n-1.

[10] IG-EPN. (2015). Informe Especial del Volcán Reventador N°2, 2015. Nuevo flujo de lava en el volcán Reventador. Quito: Escuela Politecnica Nacional. Instituto Geofisico. Retrieved 5 March 2017 from: http://www.igepn.edu.ec/reventador-informes/rev-especiales/rev-e-2015/12900-infespreventador2-19mayo2015/file.

[11] IG-EPN. (2015). Informe Especial del Volcán Reventador N°3, 2015. Intensa actividad en el volcán Reventador. Quito: Escuela Politecnica Nacional. Instituto Geofisico. Retrieved 5 March 2017 from: http://www.igepn.edu.ec/reventador-informes/rev-especiales/rev-e-2015/13046-infespreventador3-24junio2015/file.

[12] INECEL. (1988). Estudio Vulcanológico De "El Reventador". Quito: Instituto Ecuatoriano De Electrificación.

[13] James, M., Lane, S., & Chouet, B. (2006). Gas slug ascent through changes in conduit diameter: Laboratory insights into a volcano-seismic source process in low-viscosity magmas. Journal of Geophysical Research, Vol. 111, doi: 10.1029/2005JB003718, 1-25.

[14] Jaupart, C., & Vergniolle, S. (1988). Laboratory models of Hawaiian and Strombolian eruptions. Nature, 331, 58-60.

[15] Johnson, J. (2001). Generation and Propagation of Infrasonic Airwaves from Volcanic Explosions. Washington: Journal of Volcanology and Geothermal Research.

[16] Johnson, J. B. (2000). Interpretation Of Infrasound Generated By Erupting Volcanoes And Seismo-Acoustic Energy Partitioning During Strombolian Explosions. Washington: UMI. University of Washington.

[17] Johnson, J., & Aster, R. (2005). Relative partitioning of acoustic and seismic energy during Strombolian eruptions. Journal of Volcanology and Geothermal Research N.148, 334-354.

[18] Johnson, J., Harris, A., Sahetapy-Engel, S., Wolf, R., & Rose, W. (2004). Explosion dynamics of pyroclastic eruptions at Santiaguito Volcano. Geophysical Research Letters, VOL. 31, L06610, doi:

10.1029/2003GL019079, 1-5.
[19] Johnson, J., Ruiz, M., Lees, J., & Ramon, P. (2005). Poor scaling between elastic energy release and eruption intensity at Tungurahua Volcano, Ecuador. Geophysical Research Letters, Vol. 32, L15304, doi: 10.1029/2005GL022847, 1-5.
[20] McNutt, S. (1986). Observations and Analysis of B-type Earthquakes, Explosions, and Volcanic Tremor at Pavlof Volcano, Alaska. Bulletin of the Seismological Society of America, 153-175.
[21] McNutt, S. (2000). Volcanic Seismicity. In H. Sigurdsson, B. Houghton, S. McNutt, H. Rymer, & J. Stix, Encyclopedia Of Volcanoes (pp. 1015-1034). Academic Press.
[22] Mori, J., Patia, H., McKee, C., Itikarai, I., Lowenstein, P., De Saint Ours, P., & Talai, B. (1989). Seismicity associated with eruptive activity at Langila Volcano, Papua New Guinea. Journal of Volcanology and Geothermal Research. Vol. 38, 243-255.
[23] Ripepe, M., Rossi, M., & Saccorotti, G. (1993). Image processing of explosive activity at Stromboli. Journal of Volcanology and Geothermal Research. 54, 335-351.
[24] Ruiz, M. (2003). Harmonic tremor from Erebus Volcano, MS Thesis. Socorro: New Mexico Institute of Mining and Technology.
[25] Sánchez, C., Álvarez, B., Melo, F., & Vidal, V. (2014). Experimental modeling of infrasound emission from slug bursting on volcanoes. Geophysical Research Letters, Vol. 41, doi: 10.1002/2014GL061068, 6705–6711.
[26] Wassermann, J. (2002). Chapter 13. Volcano Seismology. In J. Wassermann, IASPEI New manual of seismological observatory practice (p. 42). GeoForschungs Zentrum Potsdam.
[27] Zobin, V., & Sudo, Y. (2017). Source properties of Strombolian explosions at Aso volcano, Japan, derived from seismic signals. Physics of the Earth and Planetary Interiors 268, 1-10.

Paúl I. Cornejo (M'2017). This author became a Member (M) of **World Academy of Science, Engineering and Technology** in 2017, and he was born in Quito, 14 January 1995. He obtained a Bachelor Degree at Escuela Politécnica Nacional, Quito, Ecuador in Geological Engineering, 2017.

He did an internship and also worked as Researcher at Instituto Geofísico, Escuela Politécnica Nacional (IG-EPN) during 2014 – 2016. At present, he is interested in studying about geochemistry and source magma processes.

BE. Cornejo, ex-member of the Society of Economic Geologists SEG-Student Chapter, Ecuador, and current member of the Asociación Latinoamericana de Volcanología ALVO.

Open Science Index, Geological and Environmental Engineering Vol:11, No:9, 2017 publications.waset.org/10007862/pdf